Nat. Hazards Earth Syst. Sci. Discuss., 3, 5977–6019, 2015
www.nat-hazards-earth-syst-sci-discuss.net/3/5977/2015/
doi:10.5194/nhessd-3-5977-2015

Natural Hazards and Earth System Sciences
Discussions
Open Access

Boulder accumulations related to extreme wave events on the eastern coast of Malta

S. Biolchi[1], S. Furlani[1], F. Antonioli[2], N. Baldassini[3], J. Causon Deguara[4], S. Devoto[1], A. Di Stefano[3], J. Evans[5], T. Gambin[6], R. Gauci[4], G. Mastronuzzi[7], C. Monaco[3], and G. Scicchitano[8,9]

[1]Dipartimento di Matematica e Geoscienze, Università di Trieste, Via Weiss 2, 34127 Trieste, Italy
[2]ENEA, UTMEA, Casaccia, Roma, Italy
[3]Dipartimento di Scienze Biologiche, Geologiche e Ambientali, Sezione Scienze della Terra, Università di Catania, Corso Italia 57, 95129 Catania, Italy
[4]Department of Geography, University of Malta, MSD 2080 Msida, Malta
[5]Department of Biology, University of Malta, MSD 2080 Msida, Malta
[6]Department of Classics and Archaeology, Archeology Centre, University of Malta, MSD 2080 Msida, Malta
[7]Dipartimento di Scienze della Terra e Geoambientali, Via Orabona 4, Università di Bari, 70125 Bari, Italy
[8]Dipartimento di Fisica e Scienze della Terra, Università di Messina, Viale F. Stagno D'Alcontres, 98166 Messina, Italy
[9]Geologis, Acadamic Spin Off of Dipartimento di Fisica e Scienze della Terra, Università di Messina, Messina, Italy

Received: 2 September 2015 – Accepted: 10 September 2015 – Published: 6 October 2015

Correspondence to: S. Devoto (sdevoto@units.it.)

Published by Copernicus Publications on behalf of the European Geosciences Union.

Abstract

The accumulation of large boulders related to waves generated either by tsunamis or extreme storm events has been observed in different areas of the Mediterranean Sea.

Along the NE and E low-lying rocky coasts of Malta tens of large boulder deposits have been surveyed, measured and mapped. These boulders have been detached and moved from the seafloor and lowest parts of the coast by the action of sea waves. In the Sicily–Malta channel, heavy storms are common and originate from the NE and NW winds. Conversely, few severe earthquakes and tsunamis are recorded in historical documents to have hit the Maltese archipelago, originated by seismicity activity related mainly to the Malta Escarpment, the Sicily Channel Rift Zone and the Hellenic Arc.

We present a multi-disciplinary study, which aims to define the characteristics of the boulder accumulations along the eastern coast of Malta, in order to assess the coastal geo-hazard implications triggered by the sheer ability of extreme waves to detach and move large rocky blocks inland.

The wave heights required to transport coastal boulders were calculated using various hydrodynamic equations. Particular attention was devoted to the quantification of the input parameters required in the workings of these equations. The axis sizes of blocks were measured with 3-D digital photogrammetric techniques and their densities were obtained throughout the use of a N-type Schmidt Hammer. Moreover, AMS ages were obtained from selected marine organisms encrusted on some of the boulders in various coastal sites.

The combination of the results obtained by hydrodynamic equations and the radiocarbon dating suggests that the majority of the boulders has been detached and moved by intense storm waves. Nonetheless, it is possible that some of them may have been transported by tsunami.

1 Introduction

The central part of Mediterranean Sea often experiences strong winds and high waves related to marine storms, which are common during both the winter and autumn seasons. In recent years they are being linked to an increase in the occurrence of violent "tropical like cyclones" events (Emanuel, 2005; Fita et al., 2007; Lionello et al., 2006). Such type of storm waves may represent a severe geo-hazard for inshore facilities and related land use development, as evidenced by the recent impact of severe storms on the coasts of Apulia (southern Italy) which caused extensive flooding both on Ionian and Adriatic sides. In historical and recent times, tsunami of impressive heights have been recorded to have hit some parts of the Mediterranean coasts. The 1908 earthquake-generated tsunami that struck the coasts of Calabria and Sicily in Southern Italy, developed waves up to 13 m a.s.l. destroying everything and determining tens of thousands of casualties. Most recently, the 2006 collapse of Sciarra del Fuoco along the flanks of Stromboli volcano generated large waves that destroyed harbour structures and other facilities situated on the island and along the adjacent coasts of Calabria and Sicily (i.e. Mastronuzzi et al., 2013a).

One of the most impressive evidence of extreme wave impact on the Mediterranean coasts is represented by the occurrence of mega-boulders, sparse or in field or berms whose accumulations have been attributed both to tsunamis and storm events (Mastronuzzi and Sansò, 2000, 2004; Mastronuzzi et al., 2007; Scicchitano et al., 2007, 2012; Vacchi et al., 2012; Raji et al., 2015). Notwithstanding the impressive growth in the last fifty years of studies aimed to develop an appropriate methodology, which may (in the absence of field witnesses) link these boulder deposits to a well-defined process (Williams and Hall, 2004; Hall et al., 2006; Mastronuzzi et al., 2006; Scheffers and Scheffers, 2006; Pignatelli et al., 2009; Goto et al., 2010), no undisputed consensus has yet been reached on how to differentiate between the boulders accumulated by a sea storm from those deposited by a tsunami. Some studies point to the presence of boulders and their size, to evaluate the characteristics of the impacting waves (i.e. Mastronuzzi and Pignatelli (2012), Mastronuzzi et al. (2013b) and references therein). An important degree of uncertainty lies in this methodology due to the definition of the origin of the wave responsible for the deposition of the boulders. The hydrodynamics of boulder emplacement and transport on shore platform have been dealt with, among others, by Nott (1997, 2003) and Noormets et al. (2004). Nott attributes the force required to transport boulders to wave height and proposes a straightforward method to determine if storm or tsunami waves are responsible for their emplacement. In the equation developed by Noormets, hydrodynamic forces at the low submerged shoreline cliff are computed using design wave characteristics, based on linear wave theory and experimental results and includes also the local wave climate, near-shore bottom topography and initial fracturing of cliff rocks. More recently, research attention has shifted its focus on the role of impacting wave height compared to the wave length and to the wave period. Different theories have been proposed (Goto et al., 2007, 2009; 2010; Hansom et al., 2008; Imamura et al., 2008; Pignatelli et al., 2009; Nandasena et al., 2011), suggesting that in order to evaluate the wave impact on a rocky coast, these parameters should be considered all together.

The northern coast of the island of Malta is characterised by the occurrence of deposits of anomalous calcareous boulders (Furlani et al., 2011; Mottershead et al., 2014; Causon Deguara, 2015). Their surface is frequently covered by biogenic encrustations, which indicate without any doubt that they were detached from the mid or sub-littoral zone. The aims of this paper are to identify the physical processes responsible for the accumulation of the boulders and to evaluate the vulnerability level of these Maltese coasts due to their exposure to such high-energy waves.

2 The study area

The Maltese archipelago is located in the Sicily–Malta Channel (central Mediterranean Sea), 90 km South of Sicily and 290 km North of Libyan coasts, and consists of three main islands, namely Malta (245.7 km^2), Gozo (67.1 km^2) and Comino (2.8 km^2).

From a geo-tectonic point of view, together with the Hyblean Plateau (SE Sicily), the archipelago belongs to the Pelagian Block (Grasso and Pedley, 1985), the northernmost sector of the African plate, mostly composed by foreland Neogene carbonate successions (Patacca et al., 1979). Eastwards, the Pelagian block is bounded by the Malta Escarpment, a Mesozoic passive margin separating the continental domain from the oceanic crust of the Ionian basin (Scandone et al., 1981; Makris et al., 1986). Since the Middle Pleistocene, it has been locally reactivated by normal faulting (Argnani and Bonazzi, 2005), related to a regional WNW–ESE oriented extension (Monaco et al., 1997; Bianca et al., 1999; Palano et al., 2012) (Fig. 1). It is marked by a high level of crustal seismicity producing earthquakes with intensities of up to XI-XII MCS and $M \sim 7$, such as the 1169, 1693 and 1908 events (Baratta, 1901; Postpischl, 1985; Boschi et al., 1995).

The Sicily–Malta Channel has undergone transtensional processes during the Neogene-Quaternary times, which led to the development of the Pantelleria, Linosa and Malta grabens, partially filled by Pliocene–Pleistocene sediments (Finetti, 1984). These structures are mostly bounded by NW–SE trending sub-vertical conjugate normal faults (Fig. 1), whose activity would have reached the acme approximately 5 Ma. Reactivation of the fault systems has accommodated SW-NE extension in the late Quaternary (Corti et al., 2006; Catalano et al., 2009). As revealed by available seismic database (INGV, http://emidius.mi.ingv.it/DBMI11), the above-cited structural features are the source of moderate seismicity, mostly located in the Linosa graben, with shallow events ($h < 25$ km) and magnitude usually from 2 to 4 (Civile et al., 2008).

Several earthquake-generated tsunamis struck the Ionian coast of south-eastern Sicily and the Maltese Archipelago in historical times such as in AD 1169, 1693 and 1908 (Tinti et al., 2004).

According to published geological data and numerical modelling, the seismogenic source of these events should be located in the Messina Straits and in the Ionian offshore (the Malta Escarpment) between the towns of Catania and Siracusa (e.g. Piatanesi and Tinti, 1998; Bianca et al., 1999; Monaco and Tortorici, 2000; Azzaro and

Barbano, 2000). On the other hand, we must consider that several tsunami crossed the Mediterranean Sea having been generated in the Hellenic arc area (i.e. Vött et al. (2010), Mastronuzzi et al. (2014) and references therein).

From a geomorphological point of view, the southern and western sector of the Malta island are characterised by sub-vertical cliffs increasing in height northwards (mean heights of 100–120 m in the southern tract, and of 200–225 m along the western coast of the island, close to the Great Fault). Low-lying coasts are dominant on the eastern and north-eastern part of Malta, showing a system of surf bench and wave-cut platforms which host boulders accumulations. This difference in the morphology is linked to the development of a northeastwards tilting in response to the fault system activity, also responsible for the forcing of the surface waters in a WSW–ENE direction and the formation of NE oriented fluvial valleys (Alexander, 1988; Biolchi et al., 2015). Wide sectors of NW coast of Malta are characterised by the presence of extensive landslides, mainly rock spreads and block slides (Devoto et al., 2012, 2013; Piacentini et al., 2015). These slow-moving landslides detach and move hundreds of limestone blocks from the karst plateaus towards the sea, forming peculiar coastal landforms named Rdum by locals. Conversely, slow-moving landslides and related slope-failure accumulations are not common in the NE coast, although rock spreads and block slides have been recognised and investigated in the northern side of Xemxija Bay by Panzera et al. (2012).

The submerged landscape is mainly composed of flat to gently sloping terrain and comprises coastal landforms, such as fault related scarps, paleo-shore platforms, paleo-shoreline deposits and slope-failure deposits, as well as terrestrial landforms, such as river valleys, alluvial plains, karstified limestone plateaus and sinkholes (Micallef et al., 2013).

The Maltese sedimentary succession mainly consists of pelagic limestones, clayey terrains and marls, ranging from the late Oligocene to the pre-evaporitic Messinian time interval (Giannelli and Salvatorini, 1972, 1975). As illustrated in Fig. 2, it includes four formations: (1) Lower Coralline Limestone Formation (LCL), consisting of late Oligocene (Chattian; Brandano et al., 2009) bioclastic limestones subdivided into four members (Maghlaq, Attard, Xlendi and Il-Mara Members), (2) Globigerina Limestone Formation (GLO) (Foresi et al., 2011, 2014), late Oligocene to middle Miocene in age (Baldassini et al. (2013), Baldassini and Di Stefano (2015) and reference therein), consisting of pelagic marly limestones. It is subdivided, based on the occurrence of phosphoritic conglomerate beds (Baldassini and Di Stefano, 2015), into the Lower, Middle and Upper Member, (3) Blue Clay Formation (BC), middle to late Miocene in age (Giannelli and Salvatorini, 1975; Hilgen et al., 2009), (4) Upper Coralline Limestone Formation (UCL), late Miocene in age (Giannelli and Salvatorini, 1975), consisting of shallow-water bioclastic limestone deposits. It is subdivided in four members, mainly based on the size grain increasing (Ghajn Melel, Mtarfa, Tal-Pitkal and Gebel Imbark Member; Pedley et al., 1976, 1978).

Quaternary deposits are recorded in thin levels, mainly in coastal areas as infilling of incised valleys, and consist of sands and conglomerates with paleosoil intercalations.

3 Material and methods

To identify and map the boulder accumulations, field surveys were carried out along the eastern low-lying coasts of Malta (Fig. 2). Some of these sites had already been recognised and categorised by various authors: Armier Bay by Furlani et al. (2011) and Biolchi et al. (2015); Ahrax Point, Pembroke and Xghajra by Mottershead et al. (2014); and Zonqor by Causon Deguara and Gauci (2014) and Causon Deguara (2015).

The most representative boulders, in term of size, shape and distance from the coastline, were chosen for further analysis. The selected boulders included the largest observed blocks, slab-like, roughly cubic and rectangular, as well as assembled and isolated ones.

To verify if the boulders are compatible with the storm wave regime of the area or if tsunami were responsible for their detachment, transport and deposition, a hydrodynamic approach was applied in this study. In particular, the equations used were the ones developed by Pignatelli et al. (2009), Nandasena et al. (2011) and Engel and May

(2012), in order to calculate the minimum tsunami and storm wave heights required to detach a boulder from the cliff-edge (Table 1).

Direct measurements on each boulder were carried out, for size, imbrications direction and distance from the shoreline, whilst the density was determined by means of the N-type Schmidt Hammer (SH). The latter is a field instrument (Viles et al., 2011) to determine rock physical properties (intact rock strength and density) by means of non-destructive testing (Yilmaz and Sendir, 2002). Katz et al. (2000) correlated an index named Hammer Rebound (HR), which is function of the resistance of surface material hit by the SH, to density of different types of rocks. The boulder density was associated to averaged HR value assigned to each block by means of the Eq. (1):

$$\rho = 1308.2\ln(\mathrm{HR}) - 2873.9 \qquad (1)$$

where ρ is the density unit expressed in $\mathrm{kg\,m^{-3}}$.

To avoid interferences due to the occurrence of discontinuities, fossils and weathering processes, the rebound test was applied 10 times for each block investigated and only the upper 50 % has been averaged. Moreover, in order to minimize deviations that would arise from an oblique impact (Aydin and Basu, 2005), we performed field tests keeping the hammer axis perpendicular to the boulder surface (Table 2).

As the hydrodynamic approach also depends on the pre-transport environment, the most probable setting (submerged, sub-aerial, etc.) prior to transportation has been determined. Moreover, detailed submerged profiles of the four coastal sites have been carried out by direct underwater surveying.

The onshore megaboulders at each site were inspected to identify the presence of any biological encrustations, mainly of calcareous marine bioform type, which may remain attached to the boulders after emergence above sea level. When present on a boulder, such bioforms may serve as a strong indicator of the original location of the boulder in a submerged environment and which would die once the boulder is removed from its underwater environment. The taxon of these bioforms were identified in order to create an identity list of biota. The identity and ecology of the species served as a basis to draw inferences on the origin and history of the boulders and thus be of help to further corroborate the results obtained from hydrodynamic modelling.

Radiocarbon age datings on marine bioconcrections helped to reveal the deposition time-frame. They were performed by the CeDaD Laboratory (Centro di Datazione e Diagnostica of the University of Salento, Italy). The calibration is based on the dataset achievable on the website http://calib.qub.ac.uk/marine/index.html and permits to choose between different procedure. We adopted the MMHM (= Mixed Marine North Emisphere) equation with a $\delta R = 59 \pm 40$ and $\delta R = 71 \pm 50$, respectively obtained in the Tyrrhenian Sea on *Arca tetragona* species and *Cerastoderma* genus. We preferred to use the first value because of the greater ecological similarity, in particular for nourishment, with vermetids and *chthamalus*. Indeed, the genus *Arca* lives fixed on the rocky bottoms and is characterised by suspensivor behaviour. Conversely, the genus *Cerastoderma*, although shows suspensivor behaviour, occupies the infaunal niches. Furthermore, it was considered that the percentage of carbonate origin besides Continental starts from the value of δ^{13}C.

Finally, the collected field data was compared to the Maltese wave data (Malta Maritime Authority, 2003; Malta Environment and Planning Authority, 2007; http://www.capemalta.net/maria/pages/waveforecast.html), to wave data from the Catania buoy which forms part of the Italian RON (Rete Ondametrica Nazionale) and to historical catalogues of earthquakes and tsunamis (Tinti et al., 2004; Fago et al., 2014; Papadopoulos et al., 2014) in order to make a possible correlation with known events.

4 Results

4.1 Armier Bay–Ahrax Point

This boulder site was identified for the first time by Furlani et al. (2011) and recently studied by Mottershead et al. (2014) and Biolchi et al. (2015) and is located in the north-eastern sector of the island (Fig. 2), which is exposed to winds blowing from West to North North West.

From a geomorphological point of view, this part of the coast can be defined as rocky low-lying coast, with an average slope of 5–6° (Said and Schembri, 2010; Fig. 3b).

The coast is entirely composed of Upper Coralline Limestone (Mtarfa Member). The bedding is sub-horizontal and has an average thickness of 50 cm. The boulders, ranging in size from decimetric to metric, are clustered in the central part of the deposited area at a distance from the coastline varying from 10 to 30 m (Fig. 3a and b). Away from the central outcrop, the boulders are more scattered in an isolated manner and their size decreases with increasing distance from sea level. The grain size distribution of boulders shows an exponential landward fining trend.

The boulders reach inland limits of up to 50 m away from the shoreline, at elevations of 8 m a.s.l. More than a hundred boulders account as total deposits (Mottershead et al., 2014; Fig. 3c). Some boulders are imbricated toward NE and are indicative of the flow direction from which they are deposited, with an orientation of the long axis of N300W. With regards to their shape, blocks in rectangular forms are more abundant as a result of local discontinuities and quarrying activity on blocks along the bedding planes, with the latter corresponding to the *c* axis of the boulders. On the exposed surface of some boulders, small karst features, such as solution pools, small pinnacles and microrills, were observed.

Underwater surveying uncovered a submerged scenario characterised by isolated boulders, both with fresh edges and/or covered by algae and populated by marine organisms, niches and fresh detachment scarps (Fig. 3d). The sea bottom is similar to the sub-aerial geomorphological setting, being characterised by a gentle sloping platform, interrupted by small scarps which correspond to the bedding planes (Fig. 3f).

A number of boulders at Armier Bay have remains of marine organisms. The most common were shells of the vermetid molluscs *Dendropoma petraeum* and *Vermetus triquetrus (triqueter?)*, together with calcareous rhodophytes. These two vermetid species are typical of the lower mediolittoral to infralittoral transition, and thus indicate that the boulders were at some point present at approximately mean sea level. This was confirmed with the presence of barnacle shells belonging to the family Chthamalidae on one of the boulders; such barnacles normally occur just above mean sea level. Shells of the vermetid gastropod *Thylacodes arenarius* and the skeletal remains of a coral belonging to the genus *Caryophyllia* were present on one of the smaller boulders. Both organisms occur in the shallow infralittoral, suggesting that this specific boulder was at one point fully submerged, probably at a depth of ~ 0.5–5.0 m. On the other hand, there were numerous boulders at Armier Bay without any adherent bioencrustations; however, this absence does not necessarily imply a non-marine origin, since only encrusting organisms cemented to the surface of the boulders, are likely to remain in place after emergence. Non-calcareous bioforms are very easily eroded away, leaving no trace on the boulders. The proposed scenario is a joint bounded submerged one.

The results of the application of the hydrodynamic equations are listed in Table 3, whereas Radiocarbon datings are listed in Table 4.

Moving eastwards, toward Ahrax Point, some tens of boulders have been deposited at relatively higher elevations. They actually represent the boulder site with the highest elevation point across the island of Malta. Some of them are scattered and isolated (Fig. 3e). Conversely, the major part are gathered and disposed forming a sort of storm-berm, which is aligned in the NW direction, at a distance from the coast varying from 10 to 40 m. Their maximum elevation is about 20 m. Locally, the boulders are imbricated toward NE.

At this site, the boulders do not have any marine encrustations and seem to have been detached from the top of the nearby cliff, which is deeply eroded and indented. A detachment scarp located at an elevation of 10 m a.s.l., seems to indicate a sub-aerial process-driven scenario. It is possible that these blocks correspond to cliff top storm deposits (CTSD), very similar to those characterised by some small karst pools including sand with marine shells, described by Hall et al. (2006).

4.2 Qawra–Bugibba

The coast between Bugibba and Qawra stretches further east from Mellieha Bay. This coastal area is exposed to strong winds and high waves triggered by the North Easterly storms known locally as “Grigal”. The cause of such large waves is the long fetch that stretches all the way to the Ionian Sea of Greece. These violent storms generally last 24 h, whilst in the successive days the sea conditions are characterised by large swell conditions, which continue to pound on the coastline from the same North easterly direction.

The rocky coastline of Bugibba consists of Lower Coralline Limestone (Xlendi Member), which outcrops at sea level as a sub-horizontal terrace, and connects, with on overlying steep cliff, 3–5 m high, of Globigerina Limestone. The boulders originate from both lithologies and are scattered, locally overlying each other, on the terrace, which in this area has an elevation of about 10 m a.s.l. (Fig. 4a). They are mainly rectangular, as a result of the orientation of three discontinuity sets, which act as lines of weakness on the terrace surface. Their sizes vary from decimetric to metric, with an *a* axis ranging from 1 to 2.5 m, while the *c* axis (which corresponds mainly with the bed thicknesses) measure from 0.5 to 1 m. The average direction of the long axis of the largest boulders is NW. The majority of these deposits have collapsed from the top of the slope, leaving niches and detachment scarps on the slope. Other boulders originate from the sea, as evidence by the presence of marine encrustations, including an aggregation of the vermetid mollusc *D. petraeum* as well as serpulid tubes. The presence of a vermetid crust at the surface, with a main discontinuity plane on the opposite face of the boulders, indicates that these deposits originally formed part of the coastline, with their surface at approximately mean sea level. They were eventually detached through wave undercutting and transported to their present location. Along the coastline, fresh detachment surfaces are clearly visible, both above and below sea level, with UAV (Unmanned Aerial Vehicle) images clearly showing pluck holes and isolated submerged boulders (Fig. 4b). Fresh impact marks both on the rock surface and on boulders, can be observed. For these boulders, a joint bounded submerged scenario is also being proposed.

The results of the hydrodynamic equations and of Radiocarbon dating on a sampled vermetid mollusc (*D. petraeum*, Fig. 4d) are listed respectively in Tables 3 and 4.

On the Qawra peninsula, the coast is gentle sloping and tens of boulders are distributed at an average elevation of 1 or 3 m (Fig. 4c). Their lithology, analogous to the previous, is made of Lower Coralline Limestone (Xlendi Member). Their distance from the coastline can reach up to 50 m and overall, the deposits are imbricated toward North.

One Radiocarbon dating test was performed on a serpulid polychaete, the latter sampled from the most distant and representative boulder (Table 4). This boulder had also cemented serpulid tubes, a skeleton of coral polyp (likely *Caryophyllia* sp.), and several bores made by lithophage bivalves (such as the date mussel *Lithophaga lithophaga*) with no shells visible in the holes. On the other hand, there were no vermetid concretions. Taken together, these observations strongly suggest that the sampled boulder was originally fully submerged, in a joint bounded submerged scenario.

4.3 Bahar ic–Caghaq

Bahar ic–Caghaq is located in the central part of the eastern coast, between Qawra and Pembroke. The wind and wave conditions that prevail in the Qawra–Bugibba area are also present here. Relatively shallow waters in close proximity to the coastline create high-energy areas with confused and violent conditions.

Along the coast where the Splash and Fun Water Park is located, a wide flat platform occurs and is composed of the highest unit of the Lower Coralline Limestone (Xlendi Member). The platform is covered by tens of metric boulders (Fig. 5a and b), which are imbricated toward NE.

Tens of boulders and several sections of the coast exhibit fresh detachment surfaces and indented contours. Impact marks due to the dragging of boulders on the platform are also still visible suggesting recent movements. As seen in Table 3, the results of the hydrodynamic equations provided values comparable with storm waves.

Some of these boulders had dense clusters of vermetid (mainly *D. petraeum*) tubes cemented together on the surface of the boulder, and with spaces infilled by the calcareous rhodophyte *Neogoniolithon brassica-florida*, together with remnants of other biota (e.g. the bivalves *Cardita calyculata* and *Chama gryphoides*) that are commonly associated with vermetid aggregations. These vermetid crusts are typical of the mediolittoral to infralittoral transition, indicating that the surface of these boulders was originally at approximately mean sea level. One of these boulders also contained bores made by the bivalve *Lithophaga lithophaga*, an upper infralittoral species. Also in this case, we propose a joint bounded submerged scenario.

The ^{14}C dating was performed made on a vermetid mollusc sample and is reported in Table 4.

Moving towards South, the lithology of the coast, as well as that of boulders, changes into Globigerina Limestone Formation. The boulder deposits extend for about 700 m and consist of hundreds of blocks, all metric in size, which have been deposited up to 30 m away from the coastline (Fig. 5c) and are imbricated mainly toward NE.

At sea level, a 2 m high scarp is present and is connected to a wide low-lying platform, with an average slope of 5°. The bedding is gently inclined toward the sea and its thickness is of about 0.50 m. The scarp contour is indented and fresh detachment surfaces and fractures are clearly visible. The boulders are all scattered on the low-lying platform, where the bedding favored the fracturing and the detachment of rock masses. Some of them are covered by marine encrustations, often very recent. These bioforms are similar to those observed on the LCL boulders slightly further north, and include vermetid crusts and associated biota. One specific small-sized boulder contained numerous bores with *Lithophaga lithophaga*, as well as serpulid and spirorbid polychaete tubes, the coralline alga *Ellisolandia elongata* and remains of the green alga *Cystoseira amentacea*, indicating that the boulder originated from the upper infralittoral region (joint bounded submerged scenario). Given that green algae are not encrusting species and rapidly eroded away, this specific boulder must have been transported out of the water during a very recent storm event.

The results of the hydrodynamic equations are listed in Table 3.

4.4 Pembroke

The surveyed area is located along the NE coast of Malta Island, a few hundred metres east of the Village of Pembroke. The same conditions of winds and waves that prevail in the Qawra–Bugibba area are also present here. Relatively shallow waters in close proximity to the coastline create high-energy areas with irregular and violent conditions.

From a geomorphological point of view, the outcrop consists of a low-lying rocky area of Lower Coralline Limestone Formation showing, in a northwards direction, the stratigraphic boundary between the Xlendi and the Attard members. Numerous boulders, most of which are imbricated toward NNE, have been measured and described. Generally they show a roughly rectangular shape, sometimes more rounded, with a more or less evident planar side corresponding to the detachment surface. The boulders are from decimetric to metric in dimension and are characterised by a longer axis on average from one meter, up to maximum values of 2.5 m and an overall thickness of less than one meter (Fig. 5d).

Most of the boulders identified in the Pembroke area are located at more than 20 m inland and are partly covered by a vermetid crust made by *D. petraeum* and the coralline alga *Neogoniolithon brassica-florida*. These crusts occur at the transition between the lower mediolittoral and upper infralittoral, and therefore represent the evidence of at least one submarine phase of these rocks with their upper surface located at approximately mean sea level (i.e. joint bounded submerged scenario). The absence of similar encrustations on the fracture planes of the boulders suggests that these originally formed part of the rocky coastline extending into the sea, and were subsequently detached and transported to their present position on land.

The results coming from the hydrodynamic equations are listed in Table 3, while the Radiocarbon dating, performed on a vermetid samples is listed in Table 4.

4.5 Zonqor

Zonqor is the southernmost location on the NE facing coast of the sites investigated in this study. The area takes the shape of a headland formed by the open coast to the left and the entrance to Marsascala Bay to the right. It consists of a gently sloping rock coast where the slope is mainly controlled by the dip of the bedding strata. The tip of the headland extends below sea level for some 500 m in an ESE direction up to a depth of −10 m, forming a long and narrow reef. The variation in water depth in the reef area causes considerable wave refraction around the headland, whilst its aspects render it susceptible to impact by waves approaching from a range of directions between the N and the SE.

The local bedrock is composed of Lower Globigerina Limestone and Lower Coralline Limestone. In this area the contact between these two layers is marked by a phosphatic nodule conglomerate bed. The exposed Globigerina is generally smooth in appearance and thickly bedded, however on the headland it is highly weathered exhibiting a number of fissures and fractures which have been filled and hardened with a red brown caliche crust. The Lower Coralline Limestone layer is exposed in some tracts, where the Globigerina layer above has been stripped off along lines of discontinuity in the bedrock.

The Zonqor area is marked by a high quantity of boulders many of which are angular and cuboidal in form (Fig. 6a). Their shape and size are determined by the joint patterns within the rock body from where they originate and range from less than 1 m to more than 8 m in length. Their average thickness varies between 40 and 80 cm depending on location and lithology. On the headland, the boulders form a number of distinct clusters and ridges. The two largest ridges measure 24 and 20 m in length and are aligned WNW–ESE (Fig. 6b). The majority of boulders in these ridges are either imbricated or aligned (*a* axis) towards the NE (Fig. 6c). Other smaller ridges and clusters show a prevalence of boulders imbricated or oriented towards the E, the ESE and the SE corresponding to the aspect of the headland in relation to their position. These boulder accumulations are found at approximately between 40 and 85 m from the shoreline.

Moving alongshore towards the NW the boulder distribution changes. A fault trending WNW–ESE has created a depression up to 6 m wide in which several tens of boulders have been entrapped at about 30 m from the shoreline. Some isolated boulders or clusters composed of a few clasts were observed landward of this fault. Further towards the NW the coast is dotted with more boulder clusters the majority of which show a NE imbrication or orientation. At the landward edge of the platform, a number of boulders form a berm that merges with a vegetated soft sediment slope originating mainly from anthropogenic infill. This is located at approximately 50 m inland.

The origin of the clasts at Zonqor seems to be principally from the supralittoral as evidenced from the number of detachment scarps and exposed joint facies in the backshore. However a small number of boulders with encrusting algae and a variety of other marine organisms (including the vermetid molluscs *D. petraeum* and *T. arenarius*, bivalves such as *C. calyculata*, *C. gryphoides* and the lithophage *Petricola lithophaga* and several serpulid polychaetes) indicate a sublittoral origin.

Storm wave impact on this site is considerable especially when wave approach is from a NE direction and wave inundation can reach several metres inland. This can be inferred from observed boulder movement following storms during which wind speeds exceeded 45 $\mathrm{km\,h^{-1}}$. One such boulder measuring 2.4 m × 1.3 m × 0.6 m was detached from the sublittoral and carried 15 m from the shoreline. The same boulder was moved a further 10 m inland and split into two parts, and the smaller part was transported once again some 14 m inland during subsequent storms.

The results coming from the hydrodynamic equations and Radiocarbon dating are listed in Tables 3 and 4.

5 Discussion

From a morphological point of view, the occurrence of low-lying rocky coasts makes the eastern coast of Malta more suitable for the accumulation of large boulders deriving by the impact of extreme waves. Moreover, the horizontal bedding, the presence of sub-vertical discontinuities and the poor geo-mechanical properties of the rocks play a crucial role in the rupture and detachment of large blocks from the coastline.

Concerning the pre-dislodgement setting of the boulders, a joint-bounded submerged scenario is the most frequent, while for the boulders at Ahrax Point and locally at Zonqor, Bugibba and Bahar ic-Caghaq, a subaerial scenario is suggested. Formerly, most of the large boulders investigated in this study must have been part of coastline edge, since they comprise rock pools from the most seaward surface, as well as vermetid colonies. Furthermore, according to eyewitness accounts, several boulders recently deposited by swell waves were dislodged, moved and transported landward. Mechanical quarrying of the boulders requires the presence of initial cracks. As a matter of fact, most of the measured boulder c and b axis correspond respectively to bed thickness and bed planes, which are smooth at the base and karstified at the top. These discontinuities favoured the detachment of regular slabs. Especially at Zonqor, the quarrying of regular shaped boulders is encouraged by the presence of sub-vertical faults and fractures, which are clearly visible also underwater.

On the other hand, at Ahrax Point, the boulders seem to have been detached from the top of the cliff, as they have not been colonized by marine organisms and the geomorphological setting includes a steep cliff very close to the deposits. These boulders are referred to as Cliff Top Storm Deposits (CTSD).

Bulk density of the boulders has been evaluated in 1694 $\mathrm{kg\,m^{-3}}$ for the Upper Coralline Limestone (outcropping only between Armier Bay and Ahrax Point), in 1841 $\mathrm{kg\,m^{-3}}$ for the Lower Coralline Limestone and in 1726 $\mathrm{kg\,m^{-3}}$ for the Globigerina Limestone.

The application of the hydrodynamic equations (Table 3) has highlighted the lack of correlation between density and volume values and the obtained results, meaning that not necessarily the larger boulders do require higher waves to be detached from the coastline edge. When comparing the results, it can be observed that Nandasena et al. (2011) and Pignatelli et al. (2009) are very similar: the highest values encountered reach 14 and 13.35 m for the equations of Nandasena and 12.8 and 12.7 m by Pignatelli; thus registering a marginal difference of slightly more than 1 m. For all the other values, the decrease of the storm wave height values, also decreases the difference between the obtained results. Out of the 77 selected boulders, 21 boulders recorded storm wave heights exceeding 8 m. Conversely, the calculated tsunami wave heights are very low and range between 3.5 (3.2 for Pignatelli) and 0.55 (0.51 for Pignatelli). Engel and May (2012) equations registered values relatively much lower, with the storm wave heights ranging from 1 to 6 m. Most of storm wave heights are congruent with those measured on the Maltese archipelago (Malta Maritime Authority, 2003; Malta Environment and Planning Authority, 2007; http://www.capemalta.net). During the stormiest months, or in Winter, the maximum recorded wave height values range between 5 and 5.5 m, with exceptional extreme events which can reach 7 m. However, we can suppose that in correspondence to the coast, the height can exceed 10 m since the superimposed effect of the sea bottom and coastline topographies can oversize the impacting waves.

In comparing their results, these equations provide values which are too different from each other, even though they take into account different parameters and sometimes consider scenarios which are distant from the real geomorphological setting. It was noticed that bulk and volume values do not influence in the same way the results when using different equations. Moreover, parameters such as the distance from the coastline, the elevation of a boulder and the local topographical characteristics of the sea bottom (with some being most impressive), are not taken into consideration. These are the reasons why, it can be concluded that the hydrodynamic approach as a stand-alone method is not sufficient to distinguish between storm and tsunami waves.

The Radiocarbon datings performed on 10 marine organisms sampled from 10 representative boulders in all the sites, together with those provided by Biolchi et al. (2015) gave back very interesting results (Table 4; Fig. 7). Amongst them, four samples support the hypothesis of recent strong storm events dated back to post 1954 AD. In particular, Zonqor Point is exposed to storms blowing from a variety of directions. The North Easterly storms batter this stretch of coastline just as they do in areas such as Qawra. However, Zonqor Point is also exposed to storms that originate from the South East – known locally as Xlokk. Such storms can blow both in winter and in summer and their strength, though not as powerful as those from the North East, can create very rough conditions in the area.

Additional proof of recent extreme waves is provided by the tracks of freshly damaged karst surface, generated by rolling/saltating boulder transport which lead directly from the fresh scarp at the terrace edge to the boulder's current position.

The other radiocarbon datings seem to be related to events occurred in a span of time ranging from the 514 ± 104 BC to the AD 1723 ± 40. They have been compared with historical events (Papadopoulos et al., 2014; Tinti et al., 2004). Our results could be tentatively referred to some tsunami events that have occurred in the Mediterranean Sea (Table 4). Among them, the most ancient are the 373 BC (West Corinth Gulf) and the 426 BC (Crete Island) for the boulder AB1 at Armier Bay, but this boulder, despite its significant size (4.2 m × 2.8 m × 0.5 m), is located very close to the the coast (15 m) and it is placed above other boulders.

The event of AD 963 of the Eastern Sicily, which is reported in the tsunami catalogue provided by Tinti et al. (2004) as "false event" could instead be tentatively proven by 2 nearby boulders at Armier Bay (AB4 and C82). The more recent events of AD 1303 (Crete Island) and, more probably the AD 1329 (Eastern Sicily) could be related to 3 nearby boulders at Armier Bay (AB2, AB6 and Q2). Moreover, the most interesting events, which have been occurred in the early modern period and have been reported in the historical accounts of Malta (De Soldanis, 1746; Galea, 2007) are the AD 1693 (Eastern Sicily) and the AD 1743 (Apulia, Lower Ionian Sea) strong earthquakes (with related tsunamis), which could be attributed to the boulders located at Bahar ic–Caghaq (B1) and Pembroke (16). Gozitan historian Agius de Soldanis writes the following event description in his 1746 accounts: “On 11 January of this year, the earth trembled and everyone was scared. The earthquake damaged the Collegiate Church and many other churches. The sea at Xlendi receded instantly and returned back with great fury like a tidal wave and with a thundering sound. At Sannat a part of the land measuring round a wejba crumbled down into the sea” (1746, p. 149).

Unfortunately, these attributions are contestable since:

a. the limits of the Radiocarbon age due to the limited number of samples and to the calibration;

b. the hydrodynamic approach seems not to confirm the hypothesis of ancient tsunamis, as the estimated values for storm wave heights are acceptable for the Maltese regime.

6 Conclusions

Along the eastern and north-eastern Maltese coasts about twenty boulder deposits occur. Reconstructing the history of these blocks and distinguishing events, such as storm waves or tsunami, play a crucial role in assessing this type of coastal geo-hazard. A detailed field surveying has been carried out along the Maltese coasts in order to identify and map all the sites in which these kind of deposits occur, to analyse in detail their characteristics, to determine their provenance and study the processes responsible of their transport from the sea to the coast.

Data suggest that these boulders testify the existence of a real hazard for the eastern and north-eastern coasts, considering the high land use development and coastal infrastructures present in proximity to the Maltese coastline on this part of the island. The frequent storms affecting the Maltese coasts are able to detach large boulders both from the coast edge and the sea bottom, and to transport them onshore. Very high waves are common. They can detach and move blocks whose volume can exceed 10 m^3. These blocks can be detached and moved inshore, or boulders can be initially overwhelmed and brought inshore only at a later time. The occurrence of recent extreme storm waves are supported by the Radiocarbon datings performed on marine organisms. Such events are likely to increase in frequency and intensity due to climate change, whilst sea level rise, even a temporary one such as that brought about by storm surge, could shift coastal processes landward and impinge on the urban areas.

The possibility that one or more tsunami events may have affected these coasts cannot be ruled out, since Radiocarbon datings of some marine organisms encrusted on the boulders surfaces have revealed ages that can be related to historical known tsunamis. In particular, at the Armier Bay site (Northern coast), there could be geomorphological evidence of the AD 963, 1329 and 1693 tsunami events, which occurred in the Eastern Sicily (Southern Italy). Conversely, at Bahar ic-Caghaq and Pembroke (Eastern coast), two boulders could be related to one of the two important tsunamis (AD 1693, Eastern Sicily or AD 1743, Apulia), which have also been reported in the historical accounts of Malta.

Thus a national risk assessment of extreme wave events will need to consider both an on-going monitoring system of storm wave events and related impacts on the low-lying urban coasts and on the other hand, the inclusion of the Maltese Islands as part of a Mediterranean-based tsunami early warning system, as part of a long-term strategic hazard management plan.

Acknowledgements. This work has been partially funded by the SIMIT Project “Integrated Civil Protection System for the Italo-Maltese Cross- Border Area” (Italia–Malta Programme-cohesion Policy), the Research Project COFIN MIUR 2010–2011 “Response of morphoclimatic system dynamics to global changes and related geomorphological hazard” and by the Flagship Project RITMARE – The Italian Research for the Sea – coordinated by the Italian National Research Council and funded by the Italian Ministry of Education, University and Research within the National Research Program 2011–2013.

The paper is an Italian contribution to IGCP project n. 588 – International Geological Correlation Programme by UNESCO-IUGS.

Finally, the authors are grateful to the Falck Family for the partial funding of research activities.

References

Alexander, D.: A review of the physical geography of Malta and its significance for tectonic geomorphology, Quaternary Sci. Rev., 7, 41–53, 1988.

Argnani, A. and Bonazzi, C.: Malta Escarpment fault zone offshore eastern Sicily: Pliocene-Quaternary tectonic evolution based on new multichannel seismic data, Tectonics, 24, 1–12, 2005.

Aydin, A. and Basu, A.: The Schmidt hammer in rock material characterization, Eng. Geol., 81, 1–14, 2005.

Azzaro, R. and Barbano, M. S.: Analysis of seismicity of Southeastern Sicily: proposal of a tectonic interpretation, Ann. Geofis., 43, 171–188, 2000.

Baldassini, N. and Di Stefano, A.: New insights on the Oligo-Miocene succession bearing phosphatic layers of the Maltese Archipelago, Ital. J. Geosci., 134, 355–366, 2015.

Baldassini, N., Mazzei, R., Foresi, L. M., Riforgiato, F., and Salvatorini, G.: Calcareous plankton bio-chronostratigraphy of the Maltese Lower Globigerina Limestone member, Acta Geol. Pol., 63, 105–135, 2013.

Baratta, M.: I Terremoti d'Italia, Arnaldo Forni, Bologna, 1901.

Bianca, M., Monaco, C., Tortorici, L., and Cernobori, L.: Quaternary normal faulting in southeastern Sicily (Italy): a seismic source for the 1693 large earthquake, Geophys. J. Int., 139, 370–394, 1999.

Biolchi, S., Furlani, S., Devoto, S., Gauci, R., Castaldini, D., and Soldati, M.: Geomorphological identification, classification and spatial distribution of coastal landforms of Malta (Mediterranean Sea), J. Maps, doi:10.1080/17445647.2014.984001, in press, 2015.

Boschi, E., Ferrari, G., Gasperini, P., Guidoboni, E., Smriglio, G., and Valensise, G.: Catalogo dei forti terremoti in Italia dal 461 a. C. al 1980, Istituto Nazionale di Geofisica, S. G. A., Roma, 1995.

Brandano, M., Frezza, V., Tomassetti, L., Pedley, M., and Matteucci, R.: Facies analysis and palaeoenvironmental interpretation of the Late Oligocene Attard Member (Lower Coralline Limestone Formation), Malta, Sedimentology, 56, 1138–1158, 2009.

Catalano, S., De Guidi, G., Lanzafame, G., Monaco, C., and Tortorici, L.: Late Quaternary deformation on the island of Pantelleria: new constraints for the recent tectonic evolution of the Sicily Channel Rift (southern Italy), J. Geodyn., 48, 75–82, 2009.

Causon Deguara, J.: A Study of Shore Deposits on the Coastline between Xghajra and Żonqor – Marsascala, Unpublished Masters of Arts dissertation, Department of Geography, University of Malta, 2015.

Causon Deguara, J. and Gauci, R.: Boulder and megaclast deposits on the south-east coast of Malta: signature of storm or tsunami event?, in: Proceedings Fifth International Symposium Monitoring on Mediterranean Coastal Areas: Problems and Measurement Techniques, 17–19 June 2014, Livorno, Italy, edited by: Benincasa, F., CNR-IBIMET, Florence, Italy, 594–603, 2014.

Civile, D., Lodolo, E., Tortorici, L., Lanzafame, G., and Brancolini, G.: Relationships between magmatism and tectonics in a continental rift: the Pantelleria Island region (Sicily Channel, Italy), Mar. Geol., 251, 32–46, 2008.

Corti, G., Cuffaro, M., Doglioni, C., Innocenti, F., and Manetti, P.: Coexisting geodynamic processes in the Sicily Channel, Geol. S. Am. S., 409, 83–96, 2006.

Cultrera, F., Barreca, G., Scarfì, L., and Monaco, C.: Fault reactivation by stress pattern reorganization in the Hyblean foreland domain of SE Sicily (Italy) and seismotectonic implications, Tectonophysics, doi:10.1016/j.tecto.2015.08.043, in press, 2015.

De Soldanis, G. P.: Il Gozo Antico-moderno e Sacroprofano, Isola Mediterranea adiacente a Malta Africana, Gozo, Malta, Manuscript National Archives, in: Gozo., Ancient and Modern Religious and Profane [English translation], edited by: Mercieca, A., Malta, Media Centre Publications, 1746.

Devoto, S., Biolchi, S., Bruschi, V. M., Furlani, S., Mantovani, M., Piacentini, D., Pasuto, A., and Soldati, M.: Geomorphological map of the NW coast of the Island of Malta, J. Maps, 8, 33–40, 2012.

Devoto, S., Biolchi, S., Bruschi, V. M., González-Díez, A., Mantovani, M., Pasuto, A., Piacentini, D., Schembri, J. A., and Soldati, M.: Landslides along the north-west coast of the Island of Malta, in: Landslide Science and Practice, Vol. 1: Landslide Inventory and Susceptibility and Hazard Zoning, edited by: Margottini, C., Canuti, P., and Sassa, K., Springer, Heidelberg, 57–64, 2013.

Emanuel, K. A.: Increasing destructiveness of tropical cyclones over the past 30 years, Nature, 436, 686–688, 2005.

Engel, M. and May, S. M.: Bonaire's boulder fields revisited: evidence for Holocene tsunami impact on the Leeward Antilles, Quaternary Sci. Rev., 54, 126–141, 2012.

Fago, P., Pignatelli, A., Piscitelli, A., Milella, M., Venerito, M., Sansò, P., and Mastronuzzi, G.: WebGIS for Italian tsunami: a useful tool for coastal planners, Mar. Geol., 35, 369–376, 2014.

Finetti, I. R.: Geophysical study of the Sicily Channel Rift Zone, Boll. Geof. Teor. Appl., 26, 3–28, 1984.

Fita, L., Romero, R., Luque, A., Emanuel, K., and Ramis, C.: Analysis of the environments of seven Mediterranean tropical-like storms using an axisymmetric, nonhydrostatic, cloud resolving model, Nat. Hazards Earth Syst. Sci., 7, 41–56, doi:10.5194/nhess-7-41-2007, 2007.

Foresi, L. M., Verducci, M., Baldassini, N., Lirer, F., Mazzei, R., Gianfranco, S., Ferraro, L., and Da Prato, S.: Integrated stratigraphy of St. Peter's Pool section (Malta): new age for the Upper Globigerina Limestone member and progress towards the Langhian GSSP, Stratigraphy, 8, 125–143, 2011.

Foresi, L. M., Baldassini, N., Sagnotti, L., Lirer, F., Di Stefano, A., Caricchi, C., Verducci, M., Salvatorini, G., Mazzei, R.: Integrated stratigraphy of the St. Thomas section (Malta Island): a reference section for the lower Burdigalian of the Mediterranean Region, Mar. Micropaleontol., 111, 66–89, 2014.

Furlani, S., Biolchi, S., Devoto, S., Saliba, D., and Scicchitano, G.: Large boulder along the NE Maltese coast: tsunami or storm wave deposits?, J. Coastal Res., 61, 470, 2011.

Galea, P.: Seismic history of the Maltese islands and considerations on seismic risk, Ann. Geophys.-Italy, 50, 725–740, 2007.

Giannelli, L. and Salvatorini, G.: I Foraminiferi planctonici dei sedimenti terziari dell'Arcipelago maltese, I. Biostratigrafia di "Blue Clay", "Green Sands" a "Upper Globigerina Limestone", Atti Società Toscana di Scienze Naturali, Memorie, Serie A, 79, 49–74, 1972.

Giannelli, L. and Salvatorini, G.: I foraminiferi planctonici dei sedimenti terziari dell'Arcipelago maltese, II. Biostratigrafia di "Blue Clay", "Greensand" e "Upper Coralline Limestone", Atti Società Toscana di Scienze Naturali, Memorie, Serie A, 82, 1–24, 1975.

Goto, K., Chavanich, S. A., Imamura, F., Kunthasap, P., Matsui, T., Minoura, K., Sugawara, D., and Yanagisawa, H.: Distribution, origin and transport process of boulders deposited by the 2004 Indian Ocean tsunami at Pakarang Cape, Thailand, Sediment. Geol., 202, 821–837, 2007.

Goto, K., Okada, K., and Imamura, F.: Characteristics and hydrodynamics of boulders transported by storm waves at Kudaka Island, Japan, Mar. Geol., 262, 14–24, 2009.

Goto, K., Okada, K., and Imamura, F.: Numerical analysis of boulder transport by the 2004 Indian Ocean tsunami at Pakarang Cape, Thailand, Mar. Geol., 268, 97–105, 2010.

Grasso, M. and Pedley, H. M.: The Pelagian Island: a new geological interpretation from sedimentological and tectonic studies and its bearing on the evolution of the Central Mediterranean region (Pelagian Block), Geol. Romana, 24, 13–33, 1985.

Hall, A. M., Hansom, J. D., Williams, D. M., and Jarvis, J.: Distribution, geomorphology and lithofacies of cliff-top storm deposits: examples from the high-energy coasts of Scotland and Ireland, Mar. Geol., 232, 131–155, 2006.

Hansom, J. D., Barltrop, N. D. P., and Hall, A. M.: Modelling the processes of cliff-top erosion and deposition under extreme storm waves, Mar. Geol., 253, 36–50, 2008.

Hilgen, F. J., Abels, H. A., Iaccarino, S., Krijgsman, W., Raffi, I., Sprovieri, R., Turco, E., and Zachariasse, W. J.: The Global Stratotype Section and Point (GSSP) of the Serravallian Stage (Middle Miocene), Episodes, 32, 152–166, 2009.

Imamura, F., Goto, K., and Ohkubo, S.: A numerical model for the transport of a boulder by tsunami, J. Geophys. Res.-Oceans, 113, CO1008, doi:10.1029/2007JC004170, 2008.

Katz, O., Reches, Z., and Roegiers, J. C.: Evaluation of mechanical rock properties using a Schmidt Hammer, Int. J. Rock Mech. Min., 37, 723–728, 2000.

Lionello, P., Bhend, J., Buzzi, A., Della-Marta, P. M., Krichak, S., Jansa, A., Maheras, P., Sanna, A., Trigo, I. F., and Trigo, R.: Cyclones in the Mediterranean region: climatology and effects on the environment, in: Mediterranean Climate Variability, edited by: Lionello, P., Malanotte-Rizzoli, P., and Boscolo, R., Elsevier, Amsterdam, 324–372, 2006.

Makris, J., Nicolich, R., and Weigel, W.: A seismic study in the western Ionian sea, Ann. Geophys., 6, 665–678, 1986,
http://www.ann-geophys.net/6/665/1986/.

Mastronuzzi, G. and Pignatelli, C.: The boulders berm of Punta Saguerra (Taranto, Italy): a morphological imprint of 4th April, 1836 Rossano Calabro tsunami?, Earth Planets Space, 64, 829–842, 2012.

Mastronuzzi, G. and Sansò, P.: Boulders transport by catastrophic waves along the Ionian coast of Apulia (southern Italy), Mar. Geol., 170, 93–103, 2000.

Mastronuzzi, G. and Sansò, P.: Large boulder accumulations by extreme waves along the Adriatic coast of southern Apulia (Italy), Quatern. Int., 120, 173–184, 2004.

Mastronuzzi, G., Pignatelli, C., and Sansò, P.: Boulder fields: a valuable morphological indicator of palaeotsunami in the Mediterranean sea, Z. Geomorphol. Supp., 146, 173–194, 2006.

Mastronuzzi, G., Pignatelli, C., Sansò, P., and Selleri, G.: Boulder accumulations produced by the 20th February, 1743 tsunami along the coast of southeastern Salento (Apulia region, Italy), Mar. Geol., 242, 191–205, 2007.

Mastronuzzi, G., Brückner, H., De Martini, P. M., and Regnauld, H.: Tsunami: from the open sea to the coastal zone and beyond, in: Tsunami: from Fundamentals to Damage Mitigation, edited by: Mambretti, S., WIT Press, Southampton, 1–36, 2013a.

Mastronuzzi, G., Capolongo, D., Ferilli, S., Marsico, A., Milella, M., Pignatelli, C., Piscitelli, A., and Sansò P.: Tsunami maximum flooding assessment in GIS environment, in: Tsunami: from Fundamentals to Damage Mitigation, edited by: Mambretti, S., WIT Press, Southampton, 61–80, 2013b.

Mastronuzzi, G., Calcagnile, L., Pignatelli, C., Quarta, G., Stamatopoulos, L., and Venisti, N.: Late Holocene tsunamogenic coseismic uplift in Kerkira Island, Greece, Quatern. Int., 332, 48–60, 2014.

Micallef, A., Foglini, F., Le Bas, T., Angeletti, L., Maselli, V., Pasuto, A., and Taviani, M.: The submerged paleolandscape of the Maltese Islands: morphology, evolution and relation to Quaternary environmental change, Mar. Geol., 335, 129–147, 2013.

Monaco, C. and Tortorici, L.: Active faulting in the Calabrian arc and eastern Sicily, J. Geodyn., 29, 407–424, 2000.

Monaco, C., Tapponier, P., Tortorici, L., and Gillot, P. Y.: Late Quaternary slip rates on the Acireale-Piedimonte normal faults and tectonic origin of Mt. Etna (Sicily), Earth Planet. Sc. Lett., 147, 125–139, 1997.

Mottershead, D., Bray, M., Soar, P., and Farres, P. J.: Extreme waves events in the central Mediterranean: geomorphic evidence of tsunami on the Maltese Islands, Z. Geomorphol., 58, 385–411, 2014.

Nandasena, N. A. K., Paris, R., and Tanaka, N.: Reassessment of hydrodynamic equations: minimum flow velocity to initiate boulder transport by high energy events (storms, tsunamis), Mar. Geol., 281, 70–84, 2011.

Noormets, R., Crook, K. A. W., and Felton, E. A.: Sedimentology of rocky shorelines: 3. Hydrodynamics of megaclast emplacement and transport on a shore platform, Oahu, Hawaii, Sediment. Geol., 172, 41–65, 2004.

Nott, J. F.: Extremely high-energy wave deposits inside the Great Barrier Reef, Australia: determining the cause-tsunami or tropical cyclone, Mar. Geol., 141, 193–207, 1997.

Nott, J. F.: Waves, coastal boulder deposits and the importance of the pre-transport setting, Earth Planet. Sc. Lett., 210, 269–276, 2003.

Oil Exploration Directorate: Geological Map of the Maltese Island, Sheet 1 – Malta – Scale 1 : 25,000, Office of the Prime Minister, Malta, 1993.

Palano, M., Ferranti, L., Monaco, C., Mattia, M., Aloisi, M., Bruno, V., Cannavò, F., and Siligato, G.: GPS velocity and strain fields in Sicily and southern Calabria, Italy: updated geodetic constraints on tectonic block interaction in the central Mediterranean, J. Geophys. Res.-Sol. Ea., 117, B07401, doi:10.1029/2012JB009254, 2012.

Panzera, F., D'Amico, S., Lotteri, A., Galea, P., and Lombardo, G.: Seismic site response of unstable steep slope using noise measurements: the case study of Xemxija Bay area, Malta, Nat. Hazards Earth Syst. Sci., 12, 3421–3431, doi:10.5194/nhess-12-3421-2012, 2012.

Papadopoulos, G. A., Gràcia, E., Urgeles, R., Sallares, V., De Martini, P. M., Pantosti, D., González, M., Yalciner, A. C., Mascle, J., Sakellariou, D., Salamon, A., Tinti, S., Karastathis, V., Fokaefs, A., Camerlenghi, A., Novikova, T., and Papageorgiou, A.: Historical and pre-historical tsunamis in the Mediterranean and its connected seas: geological signatures, generation mechanisms and coastal impacts, Mar. Geol., 354, 81–109, 2014.

Patacca, E., Scandone, P., Giunta, G., and Liguori, V.: Mesozoic paleotectonic evolution of the Ragusa zone (southeastern Sicily), Geol. Romana, 18, 331–369, 1979.

Pedley, H. M., House, M. R., and Waugh, B.: The geology of Malta and Gozo, Proc. Geol. Ass., 87, 325–341, 1976.

Pedley, H. M., House, M. R., and Waugh, B.: The geology of the Pelagian Block: the Maltese Islands, in: The Ocean Basins and Margins, vol. 4B, The Western Mediterranean, edited by: Nairn, A. E. M., Kanes, W. H., and Stehli, F. G., Plenum Press, London, 417–433, 1978.

Piacentini, D., Devoto, S., Mantovani, M., Pasuto, A., Prampolini, M., and Soldati, M.: Landslide susceptibility modeling assisted by Persistent Scatterers Interferometry (PSI): an example from the northwestern coast of Malta, Nat. Hazards, 78, 681–697, 2015.

Piatanesi, A. and Tinti, S.: A revision of the 1693 eastern Sicily earthquake and tsunami, J. Geophys. Res-Sol. Ea., 103, 2749–2758, 1998.

Pignatelli, C., Sansò, P., and Mastronuzzi, G.: Evaluation of tsunami flooding using geomorphologic evidence, Mar. Geol., 260, 6–18, 2009.

Postpischl, D.: Catalogo dei terremoti italiani dall'anno 1000 al 1980, CNR, P. F. Geodinamica, Graficoop, Bologna, 239 pp., 1985.

Raji, O., Dezileau, L., Von Grafenstein, U., Niazi, S., Snoussi, M., and Martinez, P.: Extreme sea events during the last millennium in the northeast of Morocco, Nat. Hazards Earth Syst. Sci., 15, 203–211, doi:10.5194/nhess-15-203-2015, 2015.

Said, G. and Schembri, J.: Malta, in: Encyclopedia of the World's Coastal Landforms, edited by: Bird, E. C. F., Springer, Dordrecht, 751–759, 2010.

Scandone, P., Patacca, E., Radoicic, R., Ryan, W. B. F., Cita, M. B., Rawson, M., Chezar, H., Miller, E., McKenzie, J., and Rossi, S.: Mesozoic and Cenozoic rocks from the Malta Escarpment (Central Mediterranean), AAPG Bull., 65, 1299–1319, 1981.

Scheffers, A. and Scheffers, S.: Documentation of the impact of hurricane Ivan on the coastline of Bonaire (Netherlands Antilles), J. Coastal Res., 22, 1437–1450, 2006.

Scicchitano, G., Monaco, C., and Tortorici, L.: Large boulder deposits by tsunami waves along the Ionian coast of south-eastern Sicily (Italy), Mar. Geol., 238, 75–91, 2007.

Scicchitano, G., Pignatelli, C., Spampinato, C. R., Piscitelli, A., Milella, M., Monaco, C., and Mastronuzzi, G.: Terrestrial Laser Scanner techniques in the assessment of tsunami impact on the Maddalena peninsula (south-eastern Sicily, Italy), Earth Planets Space, 64, 889–903, 2012.

Tinti, S., Maramai, A., and Graziani, L.: The new catalogue of Italian Tsunamis, Nat. Hazards, 33, 439–465, 2004.

Vacchi, M., Rovere, A., Zouros, N., and Firpo, M.: Assessing enigmatic boulder deposits in NE Aegean Sea: importance of historical sources as tool to support hydrodynamic equations, Nat. Hazards Earth Syst. Sci., 12, 1109–1118, doi:10.5194/nhess-12-1109-2012, 2012.

Viles, H., Goudie, A. S., Grab, S., and Lalley, J.: The use of the Schmidt Hammer and Equotip for rock hardness assessment in geomorphology and heritage science: a comparative analysis, Earth Surf. Proc. Land., 36, 320–333, 2011.

Vött, A., Bareth, G., Brückner, H., Curdt, C., Fountoulis, I., Grapmayer, R., Hadler, H., Hoffmeister, D., Klasen, N., Lang, F., Masberg, P., May, S. M., Ntageretzis, K., Sakellariou, D., and Willershäuser, T.: Beachrock-type calcarenitic tsunamites along the shores of the eastern Ionian Sea (western Greece) – case studies from Akarnania, the Ionian Islands and the western Peloponnese, Z. Geomorphol., 54, 1–50, 2010.

Williams, D. M. and Hall, A. M.: Cliff-top megaclast deposits of Ireland, a record of extreme waves in the North Atlantic – storms or tsunamis?, Mar. Geol., 206, 101–117, 2004.

Yilmaz, I. and Sendir, H.: Correlation of Schmidt hardness with unconfined compressive strength and Young's modulus in gypsum from Sivas (Turkey), Eng. Geol., 66, 211–219, 2002.

Table 1. Hydrodynamic equations (a, b and c for major, medium and minor axis respectively; ρ_b = boulder density; ρ_w = sea water density; C_L = lift coefficient = 0.178; θ = bed slope angle; μ = coefficient of static friction = 0.65; V = boulder volume; C_D = coefficient of drag = 1.95; q = boulder area coefficient = 0.73).

Equation	Joint bounded scenario	Submerged/subaerial scenario (saltation)
Pignatelli et al. (2009) Tsunami	$H_T > \frac{0.5\,c\times\left(\frac{\rho_b}{\rho_w}-1\right)}{C_L}$	–
Pignatelli et al. (2009) Storm	$H_S > \frac{2\,c\times\left(\frac{\rho_b}{\rho_w}-1\right)}{C_L}$	–
Nandasena et al. (2011) Tsunami	$H_T > \frac{0.5\,c\times\left(\frac{\rho_b}{\rho_w}-1\right)\times(\cos\theta+\mu\mathrm{sen}\theta)}{C_L}$	$H_T \geq \frac{0.5\,c\times\left(\frac{\rho_b}{\rho_w}-1\right)\times\cos\theta}{C_L}$
Nandasena et al. (2011) Storm	$H_S > \frac{2\,c\times\left(\frac{\rho_b}{\rho_w}-1\right)\times(\cos\theta+\mu\mathrm{sen}\theta)}{C_L}$	$H_S \geq \frac{2\,c\times\left(\frac{\rho_b}{\rho_w}-1\right)\times\cos\theta}{C_L}$
Engel and May (2012) Tsunami	$H_T \geq \frac{0.5\,\mu\,V\,\rho_b}{C_D\,(a\times c\times q)\,\rho_w}$	–
Engel and May (2012) Storm	$H_S \geq \frac{2\,\mu\,V\,\rho_b}{C_D\,(a\times c\times q)\,\rho_w}$	–

Title Page
Abstract Introduction
Conclusions References
Tables Figures
◀| |▶
◀ ▶
Back Close
Full Screen / Esc
Printer-friendly Version
Interactive Discussion

Table 2. N-type Schmidt Hammer *R* values performed on boulder accumulations situated along the eastern coast of Malta. The densities of boulders were determined by formulas developed by Katz et al. (2000).

Boulder no.	Geological formation	Location	Date	Averaged HR	Density [$\mathrm{kg\,m^{-3}}$]
AB1	UCL	Armier Bay	18 May 2014	35	1780
AB2	UCL	Armier Bay	18 May 2014	37	1850
AB3	UCL	Armier Bay	18 May 2014	31	1620
AB4	UCL	Armier Bay	18 May 2014	36	1810
AB5	UCL	Armier Bay	18 May 2014	32	1660
MAS New	UCL	Armier Bay	18 May 2014	30	1580
AB7	UCL	Armier Bay	18 May 2014	32	1660
AA1	UCL	Ahrax Point	30 Jan 2015	26	1390
AA9	UCL	Ahrax Point	30 Jan 2015	31	1620
AA11	UCL	Ahrax Point	30 Jan 2015	32	1660
AA12	UCL	Ahrax Point	30 Jan 2015	43	2050
AA14	UCL	Ahrax Point	30 Jan 2015	32	1660
B1	LCL	Bahar ic-Caghaq	18 May 2014	33	1700
BIC	GLO	Bahar ic-Caghaq	30 Jan 2015	26	1390
QW1	LCL	Qawra Peninsula	29 Jan 2015	15	670
QW2	LCL	Qawra Peninsula	29 Jan 2015	34	1740
QW3	LCL	Qawra Peninsula	29 Jan 2015	38	1880
LB1	LCL	Bugibba	29 Jan 2015	33	1700
LB2	LCL	Bugibba	30 Jan 2015	41	1980
LB3	LCL	Bugibba	30 Jan 2015	44	2080
LB4	LCL	Bugibba	30 Jan 2015	31	1620
LB5	LCL	Bugibba	30 Jan 2015	37	1850
LB6	LCL	Bugibba	30 Jan 2015	42	2020
LB7	LCL	Bugibba	30 Jan 2015	41	1980
LB8	LCL	Bugibba	30 Jan 2015	34	1740
LB9	LCL	Bugibba	30 Jan 2015	33	1700
LB10	LCL	Bugibba	30 Jan 2015	43	2050
P1	LCL	Pembroke	30 Jan 2015	50	2240
P3	LCL	Pembroke	30 Jan 2015	48	2190
P4	LCL	Pembroke	30 Jan 2015	44	2080
P7	LCL	Pembroke	30 Jan 2015	44	2080
Z1	LCL	Zonqor	30 Aug 2014	29	1530
Z2	GLO	Zonqor	30 Aug 2014	33	1700
Z3	GLO	Zonqor	30 Aug 2014	33	1700
Z4	GLO	Zonqor	30 Aug 2014	34	1740
Z5	GLO	Zonqor	30 Aug 2014	34	1740
Z6	GLO	Zonqor	30 Aug 2014	34	1740
Z7	GLO	Zonqor	30 Aug 2014	33	1700
Z8	GLO	Zonqor	30 Aug 2014	38	1880
Z9	GLO	Zonqor	30 Aug 2014	34	1740
Z10	GLO	Zonqor	30 Aug 2014	34	1740
Z11	GLO	Zonqor	30 Aug 2014	34	1740
Z12	GLO	Zonqor	30 Aug 2014	28	1490
Z13	GLO	Zonqor	30 Aug 2014	37	1850
Z14	Mixed	Zonqor	30 Aug 2014	35	1780
Z15	Mixed	Zonqor	30 Aug 2014	40	1950

Table 3. Physical parameters of the boulders and results of the application of the hydrodynamic equations provided by Nandasena et al. (2011), Pignatelli et al. (2009) and Engel and May (2012).

SITE	Boul-der	ax *a* (m)	ax *b* (m)	ax *c* (m)	volume (m^3)	density (g cm^{3-})	Nandasena tsunami (m)	Nandasena storm (m)	Pignatelli tsunami (m)	Pignatelli storm (m)	Engel tsunami (m)	Engel storm (m)
Ahrax Point	AA1	4.1	2.4	1.1	10.82	1.39	1.18	4.71	1.11	4.46	0.80	3.21
	AA2	2.8	1.2	1.1	3.70	1.70	2.18	8.71	2.06	8.24	0.49	1.97
	AA3	1.8	0.8	0.8	1.15	1.70	1.58	6.34	1.50	5.99	0.33	1.31
	AA4	3	2.2	0.65	4.29	1.70	1.29	5.15	1.22	4.87	0.90	3.61
	AA5	2.25	1.9	0.3	1.28	1.70	0.59	2.38	0.56	2.25	0.78	3.11
	AA7	1.7	1	0.8	1.36	1.70	1.58	6.34	1.50	5.99	0.41	1.64
	AA8	2	1	0.5	1.00	1.70	0.99	3.96	0.94	3.75	0.41	1.64
	AA9	2	1.2	0.45	1.08	1.62	0.78	3.13	0.74	2.96	0.47	1.87
Armier Bay	AB1	4.2	2.8	0.5	5.88	1.78	1.10	4.41	1.04	4.17	1.20	4.80
	AB2	3.5	1.6	0.55	3.08	1.85	1.33	5.32	1.26	5.03	0.71	2.85
	AB3	2	1.6	0.8	2.56	1.62	1.39	5.57	1.32	5.27	0.62	2.50
	AB4	1.9	1.4	1.4	3.72	1.81	3.24	12.95	3.06	12.24	0.61	2.45
	AB6	1.6	1.2	0.5	0.96	1.70	0.99	3.96	0.94	3.75	0.49	1.97
	AB7	3.4	1.6	1.15	6.26	1.70	2.28	9.11	2.15	8.61	0.66	2.62
	C16	0.9	0.8	0.25	0.18	1.80	0.57	2.27	0.54	2.15	0.35	1.39
	C82/AB5	2.56	1.06	0.92	2.50	1.70	1.82	7.29	1.72	6.89	0.43	1.74
	new	2.39	1.69	0.82	3.31	1.58	1.33	5.31	1.26	5.02	0.64	2.57
	Q2	0.75	0.55	0.5	0.21	1.70	0.99	3.96	0.94	3.75	0.23	0.90
Bahar Ic Caghaq	B1	2.3	0.6	0.36	2.55	1.70	1.14	4.55	1.12	4.49	0.76	3.03
	B10	3.1	1.6	0.6	2.98	1.39	0.66	2.62	0.61	2.43	0.54	2.14
	B11	3.3	1.8	0.69	4.10	1.39	0.75	3.01	0.70	2.80	0.60	2.41
	B12	3.1	2.35	0.5	3.64	1.39	0.55	2.18	0.51	2.03	0.79	3.15
	B13	4.3	3.4	0.7	10.23	1.39	0.76	3.06	0.71	2.84	1.14	4.55
	B14	3.2	2.1	1.1	7.39	1.39	1.20	4.81	1.11	4.46	0.70	2.81
	B2	4.35	3.65	0.4	6.35	1.80	0.87	3.48	0.86	3.44	1.58	6.33
	B3	2.4	1.8	0.55	2.38	1.80	1.20	4.78	1.18	4.73	0.78	3.12
	B4	2.6	1.7	0.7	3.09	1.80	1.52	6.09	1.50	6.01	0.74	2.95
	B5	2.15	1.93	0.7	2.90	1.80	1.52	6.09	1.50	6.01	0.84	3.35
	B6	2	1.5	0.55	1.65	1.80	1.20	4.78	1.18	4.73	0.65	2.60
	B7	2.3	1.6	0.36	1.32	1.80	0.78	3.13	0.77	3.09	0.69	2.78
	B8	3	2.4	1	7.20	1.80	2.17	8.70	2.15	8.59	1.04	4.17
	B9	3.3	1.65	0.6	3.27	1.39	0.66	2.62	0.61	2.43	0.55	2.21
Bugibba	LB1	4	2	1.2	9.60	1.70	2.44	9.78	2.25	8.99	0.82	3.28
	LB10	2.4	2.3	0.5	2.76	2.05	1.50	5.98	1.41	5.66	1.13	4.54
	LB2	2.9	1.65	1.05	5.02	1.98	3.03	12.13	2.79	11.15	0.79	3.16
	LB3	2.6	1.8	1.1	5.15	2.08	3.54	14.17	3.20	12.81	0.90	3.60
	LB4	3.3	2.8	0.6	5.54	1.62	1.09	4.37	0.99	3.95	1.09	4.37
	LB6	2.016	1.12	0.35	0.79	1.85	0.89	3.54	0.80	3.20	0.50	2.00
	LB7	1.984	1.8	1.1	3.93	2.02	3.34	13.35	3.02	12.07	0.87	3.50
	LB8	1.739	1.6	0.85	2.37	1.74	1.86	7.45	1.68	6.73	0.67	2.68
	LB9	2.5	2.15	0.8	4.30	1.70	1.63	6.52	1.50	5.99	0.88	3.52

Title Page
Abstract Introduction
Conclusions References
Tables Figures
◀| |▶
◀ ▶
Back Close
Full Screen / Esc
Printer-friendly Version
Interactive Discussion

Title Page
Abstract
Introduction
Conclusions
References
Tables
Figures
◀|
|▶
◀
▶
Back
Close
Full Screen / Esc
Printer-friendly Version
Interactive Discussion

Table 3. Continued.

SITE	Boulder	ax *a* (m)	ax *b* (m)	ax *c* (m)	volume (m^3)	density ($g\,cm^{-3}$)	Nandasena tsunami (m)	Nandasena storm (m)	Pignatelli tsunami (m)	Pignatelli storm (m)	Engel tsunami (m)	Engel storm (m)
Qawra	Qa1	1.8	1.4	1.3	3.28	1.80	2.95	11.81	2.79	11.17	0.61	2.43
	Qa2	2.2	1.2	0.65	1.72	1.80	1.54	6.18	1.40	5.58	0.52	2.08
	Qa3	1.5	1.5	0.7	1.58	1.85	1.77	7.08	1.60	6.40	0.67	2.68
	qawra_2	2	1.05	0.6	1.26	1.74	1.24	4.97	1.19	4.75	0.44	1.76
	qawra_3	2.3	1.5	1.1	3.80	1.88	2.74	10.95	2.62	10.47	0.68	2.72
Pembroke	P1	2.55	1.2	0.6	1.84	2.24	2.18	8.72	2.02	8.09	0.65	2.60
	P10	2.55	1.5	0.35	1.34	2.08	1.07	4.26	1.02	4.08	0.75	3.00
	P16	2	1.3	0.4	1.04	1.80	0.90	3.60	0.86	3.44	0.56	2.26
	P2	2	1.5	0.65	1.95	2.20	2.28	9.11	2.11	8.45	0.80	3.18
	P3	2.85	2.7	0.8	6.16	2.19	2.78	11.11	2.58	10.31	1.43	5.70
	P4	2.5	1.8	0.7	3.15	2.08	2.20	8.79	2.04	8.15	0.90	3.60
	P5	2.8	1.5	0.7	2.94	2.08	2.20	8.79	2.04	8.15	0.75	3.00
	P6	2.4	2.1	0.7	3.53	2.08	2.20	8.79	2.04	8.15	1.05	4.21
	P7	2.55	1.4	0.5	1.79	2.08	1.52	6.09	1.46	5.82	0.70	2.80
	P9	2.55	1.5	0.6	2.30	2.08	1.83	7.31	1.75	6.99	0.75	3.00
Zonqor	Z1	2.8	2.2	0.8	4.93	1.53	1.17	4.66	1.13	4.50	0.81	3.25
	Z10	4.1	2.2	0.7	6.31	1.74	1.47	5.86	1.39	5.54	0.92	3.69
	Z11	5.3	2.6	1.5	20.67	1.74	3.20	12.81	2.97	11.88	1.09	4.36
	Z12	2.3	1.2	0.7	1.93	1.49	0.97	3.86	0.90	3.59	0.43	1.72
	Z13	2.4	0.86	0.7	1.44	1.85	1.72	6.90	1.60	6.40	0.38	1.53
	Z14	5.1	1.55	1	7.91	1.78	2.25	8.99	2.08	8.34	0.66	2.66
	Z15	2.8	1.1	1	3.08	1.75	2.17	8.69	2.02	8.06	0.46	1.86
	Z2	2.7	1.8	0.5	2.43	1.70	0.97	3.88	0.94	3.75	0.74	2.95
	Z3	3.3	2.8	0.9	8.32	1.70	1.83	7.33	1.69	6.74	1.15	4.59
	Z4	4.35	3	0.7	9.14	1.74	1.51	6.03	1.39	5.54	1.26	5.03
	Z5	2.6	1.5	0.7	2.73	1.74	1.51	6.03	1.39	5.54	0.63	2.52
	Z6	8.5	4	1.2	40.80	1.74	2.46	9.84	2.38	9.50	1.68	6.71
	Z7	3.45	1.45	0.7	3.50	1.70	1.36	5.43	1.31	5.24	0.59	2.38
	Z8	3.3	2.2	0.7	5.08	1.88	1.76	7.04	1.67	6.66	1.00	4.00
	Z9	3.1	1.45	1	4.50	1.74	2.09	8.37	1.98	7.92	0.61	2.43

Table 4. 14C AMS datings of marine organisms performed by the CeDaD Laboratory (Centro di Datazione e Diagnostica) of the University of Salento, Brindisi, Italy. The last column lists the historical tsunamis occurred in the Mediterranean Sea in the ranges of the Radiocarbon ages (Tinti et al., 2004; Papadopoulos et al., 2014).

Boulder (site)	Calibration method	Type organism	Radiocarbon Age (BP)	δ^{13}C (‰)	Cal. Age (BC or AD)	Historical tsunamis
AB1 (Armier Bay)	1 MMNH (+)	Vermetidae (*D. petraeum*)	2784 ± 45	−2.2 ± 0.4	514 ± 104 BC	?
AB2A (Armier Bay)	2 MMHM	Vermetidae (*D. petraeum*)	1095 ± 45	−3.4 ± 0.2	AD 1298 ± 46	1329 (Eastern Sicily)
AB4A (Armier Bay)	5 MMHM	Chthamalidae	1525 ± 45	−0.5 ± 0.5	AD 938 ± 70	963 (Sicily)
AB6 (Armier Bay)	6 MMHM	Vermetidae (*D. petraeum*)	1147 ± 45	−0.5 ± 0.3	AD 1290 ± 54	1329 (Eastern Sicily)
AB7 (Armier Bay)	7 MMHM	Vermetidae (*D. petraeum*)	2229 ± 45	−4.5 ± 0.8	AD 122 ± 72	148 (Rhodes)?
C16 (Armier Bay)	–	Vermetidae (*T. arenarius*)	107.08 ± 0.60 pMC	−0.6 ± 0.5	Post 1954	
Q2 (Armier Bay)	8 Marine13.14c	Vermetidae (*V. triquetrus*)	1026 ± 45	+4.0 ± 0.5	AD 1384 ± 47	1329 (Eastern Sicily)
C82 (Armier Bay)	9 Marine13.14c	Vermetidae (*D. petraeum*)	1582 ± 45	7.4 ± 0.6	AD 869 ± 75	963 (Sicily)
Qa1 (Qawra)	–	Serpulidae	110.34 ± 0.59 pMC	−6.3 ± 0.3	Post 1954	
Qa2 (Bugibba)	–	Vermetidae (*D. petraeum*)	108.52 ± 0.55 pMC	−5.6 ± 0.6	Post 1594	
B1 (Bahar ic-Cagaq)	3 MMHM	Vermetidae (*D. petraeum*)	278 ± 45	−2.2 ± 0.6	AD 1672 ± 45	1693 (Sicily), or 1743 (Apulia)
16 (Pembroke)	4 MMHM	Vermetidae (*D. petraeum*)	227 ± 40	−3.7 ± 0.5	AD 1723 ± 40	1693 (Sicily) or 1743 (Apulia)
Z1 (Zonqor)	–	Vermetidae	108.92 ± 0.53 pMC	−6.1 ± 0.4	Post 1954	

NHESSD
3, 5977–6019, 2015

Title Page
Abstract | Introduction
Conclusions | References
Tables | Figures
◀| |▶
◀ ▶
Back | Close
Full Screen / Esc
Printer-friendly Version
Interactive Discussion

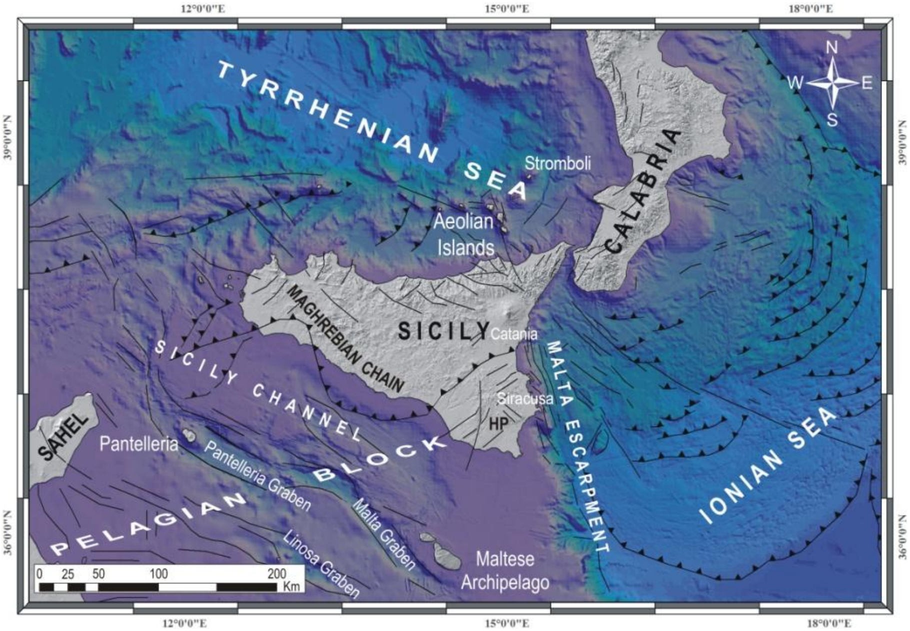

Figure 1. Geodynamical setting of the Maltese Archipelago (redrawn from Cultrera et al., 2015).

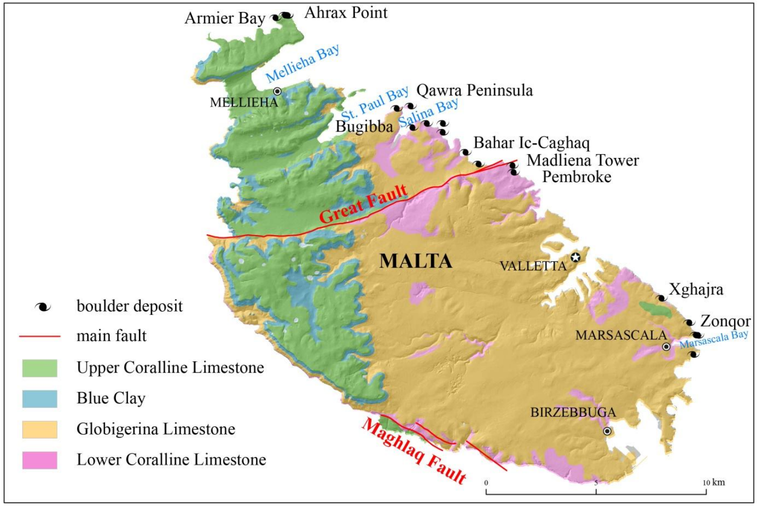

Figure 2. Geological Map of the Maltese Archipelago and location of the boulder deposits (redrawn from Oil Exploration Directorate, 1993; Devoto et al., 2012).

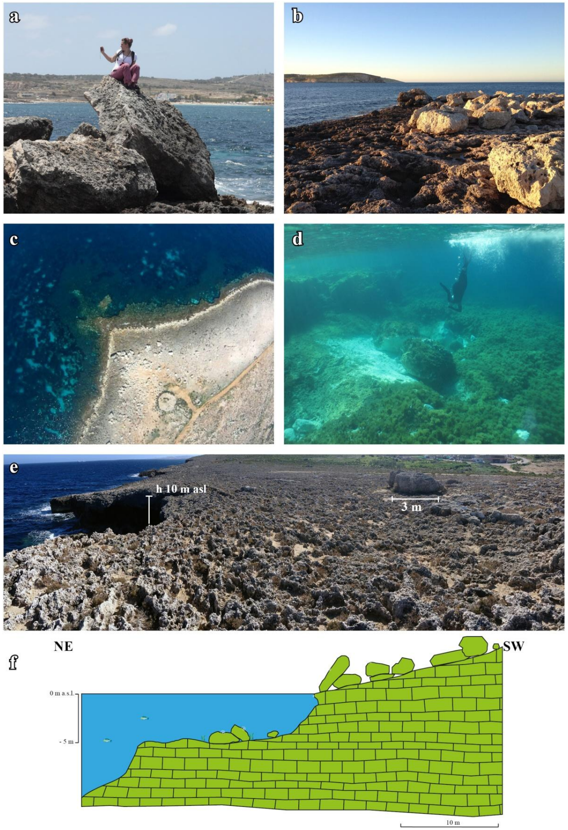

Figure 3. Armier Bay-Ahrax Point site: **(a, b)** boulders; **(c)** view of the boulder deposit from UAV (Unmanned Aerial Vehicle); **(d)** submerged isolated boulders; **(e)** cliff top storm deposits; **(f)** reconstruction of the submerged environment.

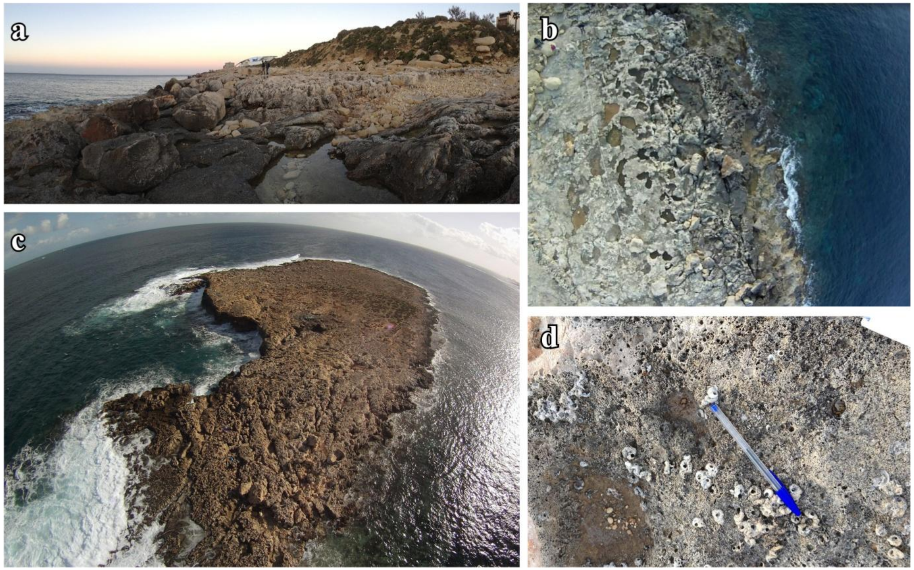

Figure 4. (a) Boulder deposit at Bugibba; **(b)** view of the deposit from UAV; **(c)** view of Qawra peninsula from UAV; **(d)** Vermetid shells.

Title Page
Abstract Introduction
Conclusions References
Tables Figures
◀| |▶
◀ ▶
Back Close
Full Screen / Esc

Printer-friendly Version
Interactive Discussion

Figure 5. Splash and Fun Water Park: **(a)** scattered boulders belonging to LCL; **(b)** UAV view of the deposit; **(c)** Bahar ic–Caghaq: boulders belonging to GL; **(d)** isolated boulders at Pembroke.

Figure 6. Zonqor: **(a, b)** boulder deposits; **(c)** fresh marine encrustations; **(d)** underwater fresh detachment surfaces along bedding and fracture planes; **(e)** submerged rectangular and rounded metric boulders; **(f)** reconstruction of the submerged environment.

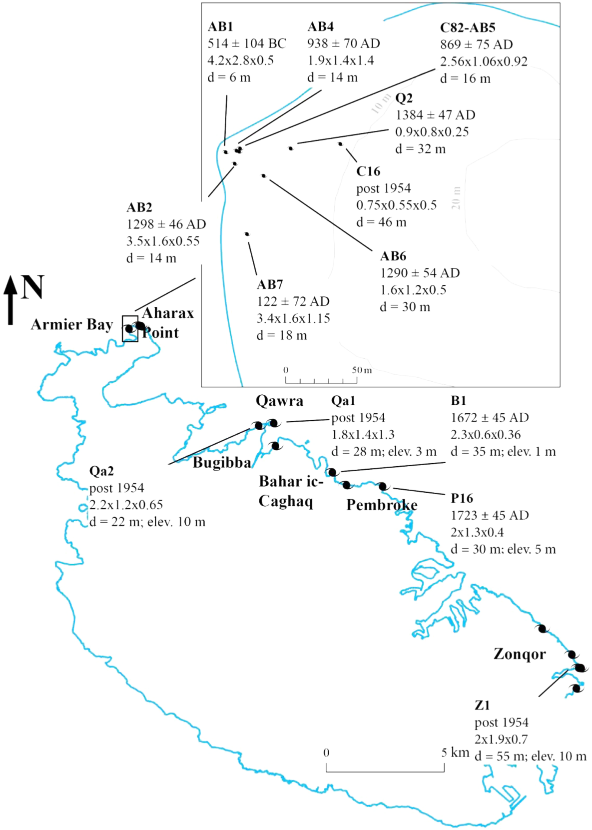

Figure 7. Location of the investigated boulders with zoom on Armier Bay-Ahrax Point site with their AMS dating, size, distance from the coastline and elevation a.s.l.